

## Adsorption properties of hydrazine on pristine and Si-doped $\text{Al}_{12}\text{N}_{12}$ nano-cage

Mohammad T. Baei<sup>a</sup>, Alireza Soltani<sup>b,c</sup>, and Saeedeh Hashemian<sup>d</sup>

<sup>a</sup>Department of Chemistry, Azadshahr Branch, Islamic Azad University, Azadshahr, Golestan, Islamic Republic of Iran; <sup>b</sup>Joints, Bones and Connective Tissue Research Center, Golestan University of Medical Science, Gorgan, Islamic Republic of Iran; <sup>c</sup>Young Researchers and Elite Club, Gorgan Branch, Islamic Azad University, Gorgan, Islamic Republic of Iran; <sup>d</sup>Department of Chemistry, Yazd Branch, Islamic Azad University, Yazd, Islamic Republic of Iran

### ABSTRACT

The interaction of hydrazine ( $\text{N}_2\text{H}_4$ ) molecule with pristine and Si-doped aluminum nitride ( $\text{Al}_{12}\text{N}_{12}$ ) nano-cage was investigated using the density functional theory calculations. The adsorption energy of  $\text{N}_2\text{H}_4$  on pristine  $\text{Al}_{12}\text{N}_{12}$  in different configurations was about  $-1.67$  and  $-1.64$  eV with slight changes in its electronic structure. The results showed that the pristine nano-cage can be used as a chemical adsorbent for toxic hydrazine in nature. Compared with very low sensitivity between  $\text{N}_2\text{H}_4$  and  $\text{Al}_{12}\text{N}_{12}$  nano-cage,  $\text{N}_2\text{H}_4$  molecule exhibits high sensitivity toward Si-doped  $\text{Al}_{12}\text{N}_{12}$  nano-cage so that the energy gap of the Si-doped  $\text{Al}_{12}\text{N}_{12}$  nano-cage is changed by about 31.86% and 37.61% for different configurations in the  $\text{Si}_{\text{Al}}$  model and by about 26.10% in the  $\text{Si}_{\text{N}}$  model after the adsorption process. On the other hand, in comparison with the  $\text{Si}_{\text{Al}}$  model, the adsorption energy of  $\text{N}_2\text{H}_4$  on the  $\text{Si}_{\text{N}}$  model is less than that on the  $\text{Si}_{\text{Al}}$  model to hinder the recovery of the nano-cage. As a result, the  $\text{Si}_{\text{N}}\text{Al}_{12}\text{N}_{11}$  is anticipated to be a potential novel sensor for detecting the presence of  $\text{N}_2\text{H}_4$  molecule.

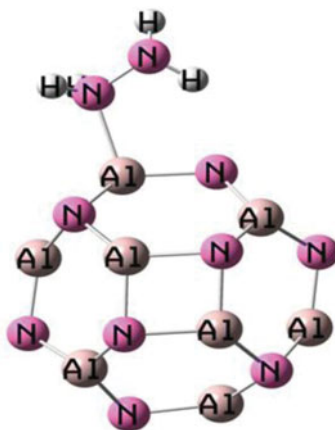
### ARTICLE HISTORY

Received 21 February 2015  
Accepted 7 July 2015

### KEYWORDS

Aluminum nitride  
nano-cage; hydrazine;  
adsorbent; sensor



### GRAPHICAL ABSTRACT



### Introduction

Hydrazine ( $\text{N}_2\text{H}_4$ ) is an inorganic compound used widely for several important applications, including rocket fuels, weapons of mass destruction, fuel cells, and missile systems.<sup>1</sup> Hydrazine is highly toxic and the lungs, liver, kidneys, and central nervous system of living organisms can be injured if inhaled or introduced in the skin. Thus, it is necessary to monitor and control important pollutants such as  $\text{N}_2\text{H}_4$  molecule in environmental systems. Owing to its toxic effects,  $\text{N}_2\text{H}_4$  adsorption has high importance in surface science.<sup>2–4</sup> So far, various reports have been published on the adsorption of  $\text{N}_2\text{H}_4$  molecule upon different adsorbate configurations. Alberas et al.<sup>5</sup> investigated the structure of adsorbed hydrazine on Pt(111) via X-ray

photoelectron spectroscopy (XPS) experiment, which showed that  $\text{N}_2\text{H}_4$  molecule is chemically adsorbed in *cis*-configuration where both nitrogen atoms are bonded to the surface. A density functional theory (DFT) investigation on the adsorption of hydrazine on Ni(100) was performed by Agusta et al.,<sup>2</sup> concluding that *anti*-configuration is the more favored configuration for the adsorption state. Recent calculations by Yu et al.<sup>6</sup> have indicated the effect of humidity upon the adsorption of hydrazine on single-walled carbon nanotubes. They found that the adsorption of hydrazine on carbon nanotubes in the presence of humidity will introduce occupied impurity states near the bottom of the conduction band in this system, leading to *n*-type behavior. The functionalization of BN nano-sheets with

**CONTACT** Mohammad T. Baei  Baei52@yahoo.com  Department of Chemistry, Azadshahr Branch, Islamic Azad University, Azadshahr, Golestan, Islamic Republic of Iran.

Color versions of one or more of the figures in the article can be found online at [www.tandfonline.com/gpps](http://www.tandfonline.com/gpps).

© 2016 Taylor & Francis Group, LLC

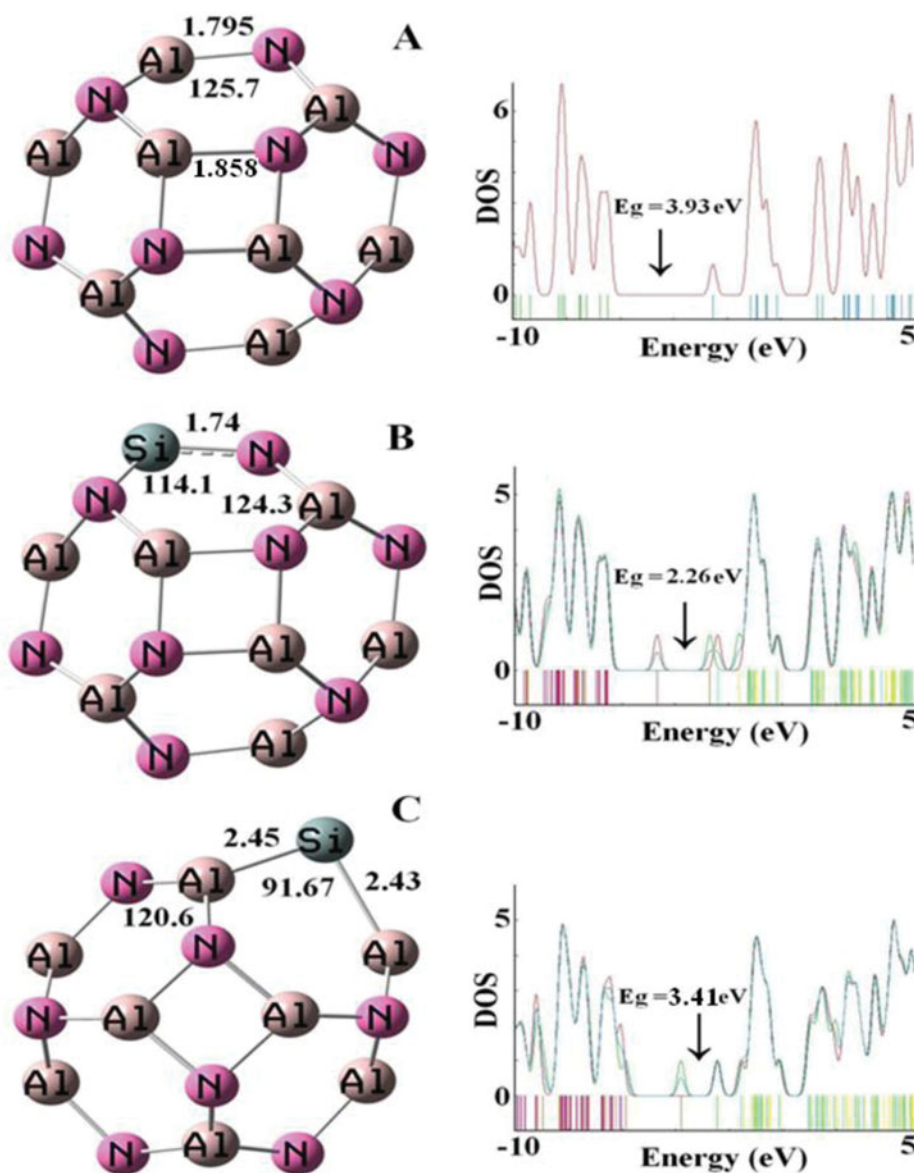


**Figure 1.** Optimized structures of pristine,  $\text{SiAl}_1$ , and  $\text{Si}_\text{N}$  models of  $\text{Al}_{12}\text{N}_{12}$  nano-cage and their density of states (bond lengths are in Å).

**Table 1.** Structural and electronic properties for different systems.

Property	$\text{N}_2\text{H}_4$	$\text{Al}_{12}\text{N}_{12}$	$\text{N}_2\text{H}_4/\text{Al}_{12}\text{N}_{12}$ (Figure 2a)	$\text{N}_2\text{H}_4/\text{Al}_{12}\text{N}_{12}$ (Figure 2b)	$\text{SiAl}_{11}\text{N}_{12}$	$\text{SiAl}_{12}\text{N}_{11}$	$\text{N}_2\text{H}_4/\text{SiAl}_{11}\text{N}_{12}$ (Figure 3a)	$\text{N}_2\text{H}_4/\text{SiAl}_{11}\text{N}_{12}$ (Figure 3b)	$\text{N}_2\text{H}_4/\text{SiAl}_{12}\text{N}_{11}$
$l_{\text{Si-N}}$	–	–	–	–	1.741	–	1.696	1.716	–
$l_{\text{Al-Si}}$	–	–	–	–	–	2.452	–	–	2.459
$l_{\text{N-Si-N}}$	–	–	–	–	114.1	–	122.8	122.8	–
$l_{\text{Al-Si-Al}}$	–	–	–	–	–	91.67	–	–	86.76
$l_{\text{N-H}}$	1.023	–	1.024	1.021	–	–	1.026	1.024	1.018
$l_{\text{N-N}}$	1.489	–	1.449	1.451	–	–	1.449	1.446	1.431
$l_{\text{H-N-H}}$	102.22	–	107.4	107.3	–	–	107.8	109.2	108.9
$D/\text{Å}$	–	–	2.038	2.040	–	–	1.972	1.973	2.431
$E_{\text{ad}}/\text{eV}$	–	–	–1.67	–1.64	–	–	–1.18	–1.23	–0.30
$E_{\text{HOMO}}/\text{eV}$	–4.47	–6.47	–6.06	–6.07	–4.68	–5.88	–3.11	–3.45	–4.64
$E_{\text{LUMO}}/\text{eV}$	–2.05	–2.54	–2.15	–2.15	–2.42	–2.47	–1.57	–2.04	–2.12
$E_{\text{g}}/\text{eV}$	4.47	3.93	3.91	3.92	2.26	3.41	1.54	1.41	2.52
$\Delta E_{\text{g}}(\%)$	–	–	0.51	0.25	–	–	31.86	37.61	26.10
$\Phi/\text{eV}$	2.24	1.96	1.96	1.96	1.13	1.70	0.77	0.70	1.26
DM/Debye	2.20	0.00	5.74	8.37	1.57	0.69	8.59	7.08	6.39
$E_{\text{F}}/\text{eV}$	–4.28	–4.50	–4.10	–4.11	–3.55	–4.18	–2.34	–2.74	–3.38

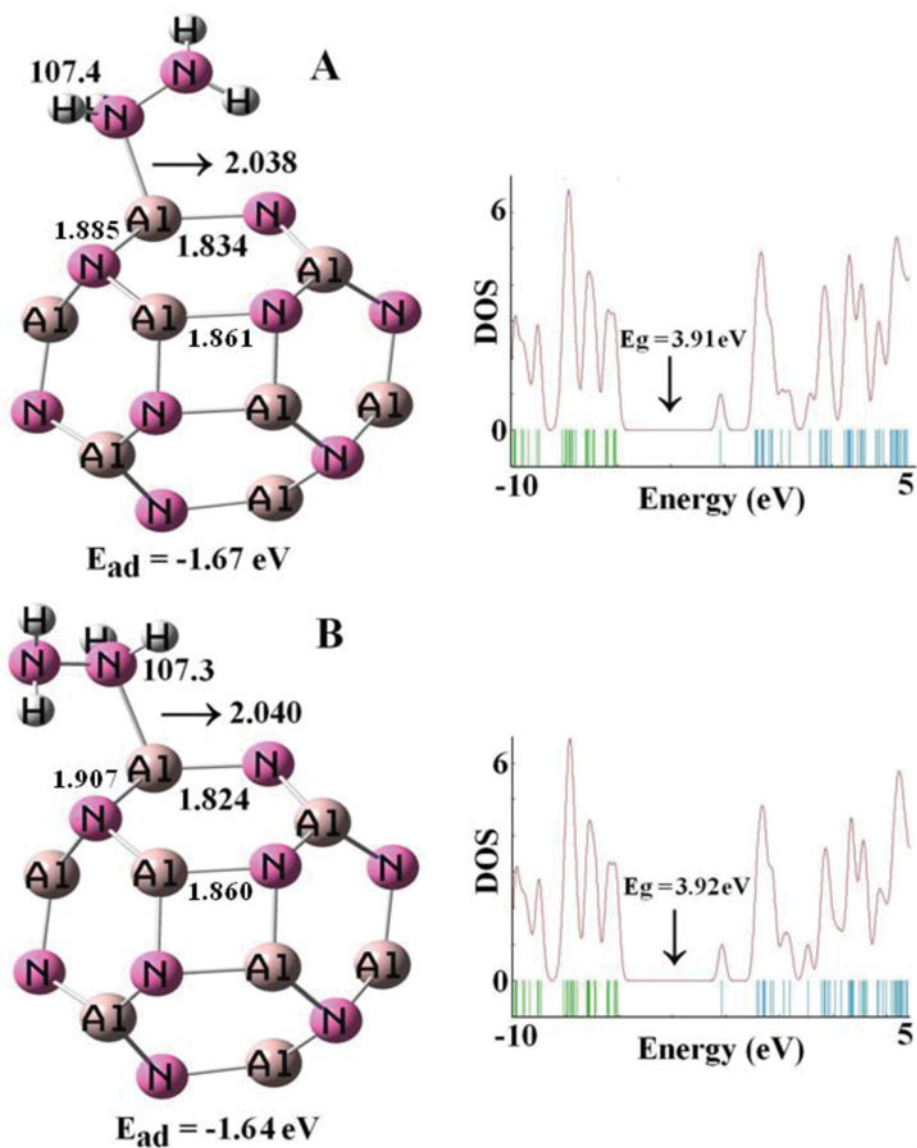


**Figure 2.** Different models of  $N_2H_4$  adsorption on the pristine  $Al_{12}N_{12}$  nano-cage and corresponding density of states.

hydrazine is reported by Beheshtian et al.,<sup>7</sup> showing that it is not possible for a  $N_2H_4$  molecule to be functionalized upon the pristine BN nano-sheet, while some structural defects such as Stone–Wales defects through the surface of adsorbate can make it conceivable. Soltani et al.<sup>8</sup> have shown that Mg-doped aluminum nitride ( $Al_{12}N_{12}$ ) exhibits high sensitivity to the presence of  $NO_2$  and  $SO_2$  molecules in comparison with Ga-doped  $Al_{12}N_{12}$  nano-cage. Recent theoretical studies have shown that AlN nano-clusters might selectively detect NO in the presence of CO.<sup>9</sup> In this article, we present detailed DFT calculations of  $N_2H_4$  adsorption on pure and Si-doped  $Al_{12}N_{12}$  nano-cage at the B3LYP level of theory using 6-31G\* basis set. In addition, stability of adsorption configurations is studied using energetic and electronic structures, molecular electrostatic potential (MEP) plot, and the Mulliken population analysis (MPA). Our results show that  $Al_{12}N_{12}$  nano-cage can be used as a chemical adsorbent for this molecule. Also,  $Si_NAl_{12}N_{11}$  nano-cage can be used as a potential novel sensor for  $N_2H_4$  molecule.

### Computational methods

The adsorption of hydrazine on pristine and Si-doped  $Al_{12}N_{12}$  was studied by means of DFT calculations at the B3LYP/6-31G\* level of theory, in particular the geometry optimizations, energy calculations, and density of state (DOS) analysis. B3LYP is a commonly used theoretical approach for the investigation of different nano-structures.<sup>10,11</sup> This method was used to calculate the adsorption energy ( $E_{ad}$ ) of hydrazine on the surface of pure and Si-doped  $Al_{12}N_{12}$  nano-cages as follows:

$$E_{ad} = E_{\text{hydrazine}/Al_{12}N_{12}} - [E_{Al_{12}N_{12}} + E_{\text{hydrazine}}] \quad (1)$$

$$E_{ad} = E_{\text{hydrazine}/SiAl_{11}N_{12}} - [E_{SiAl_{11}N_{12}} + E_{\text{hydrazine}}] \quad (2)$$

$$E_{ad} = E_{\text{hydrazine}/SiAl_{12}N_{11}} - [E_{SiAl_{12}N_{11}} + E_{\text{hydrazine}}] \quad (3)$$

where  $E_{\text{hydrazine}/Al_{12}N_{12}}$  is the total energy of a  $N_2H_4$  molecule adsorbed on  $Al_{12}N_{12}$  nano-cage,  $E_{Al_{12}N_{12}}$ ,  $E_{SiAl_{11}N_{12}}$ ,  $E_{SiAl_{12}N_{11}}$ , and  $E_{\text{hydrazine}}$  are the total energies of pristine, Si-doped  $Al_{12}N_{12}$  nano-cage, and  $N_2H_4$  molecule. Negative or positive value for

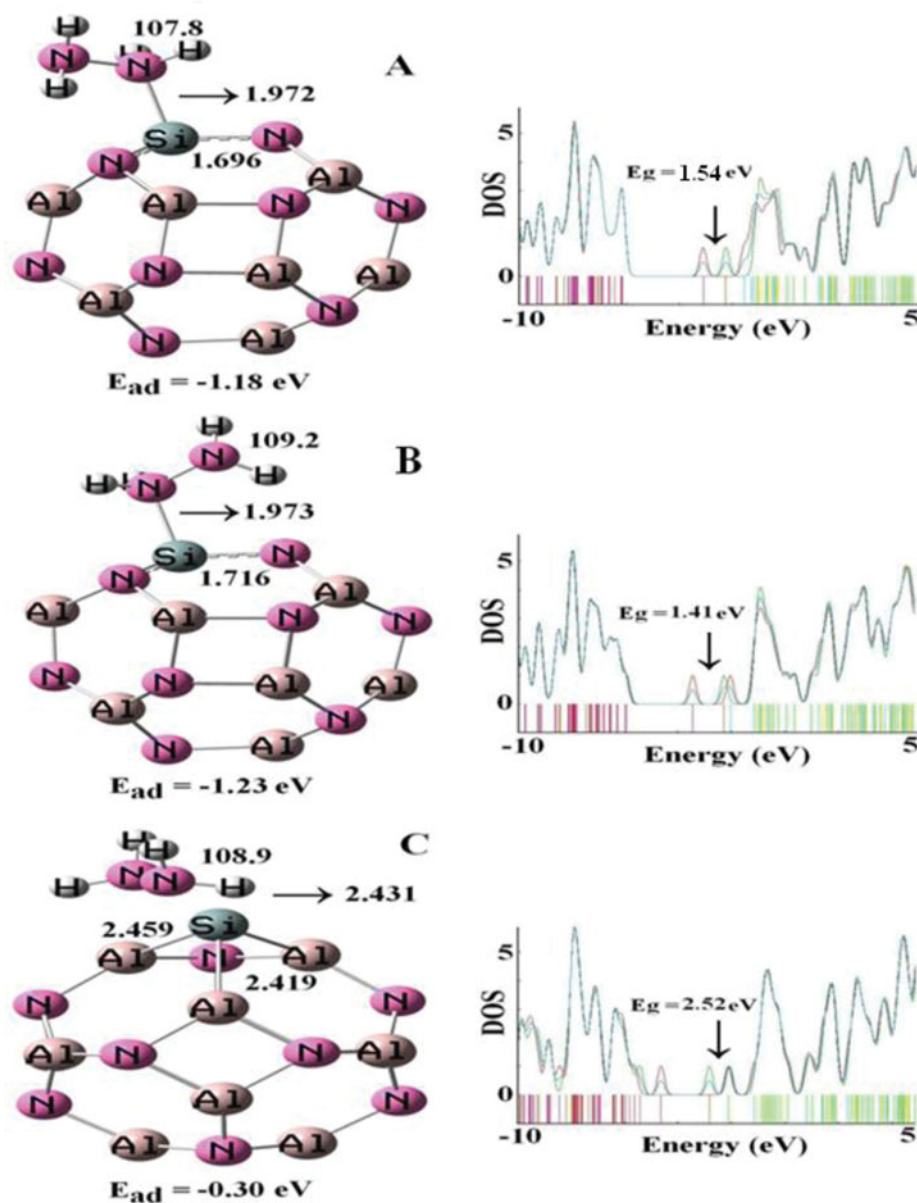


**Figure 3.** Different models of  $N_2H_4$  adsorption and their density of states on  $Si_{Al}$  and  $Si_N$  model nano-cages.

$E_{ad}$  is referred to exothermic or endothermic processes, respectively. The canonical assumption for Fermi-level energy ( $E_{FL}$ ) is a molecule at 0 K and it lies approximately in the middle of the energy gap ( $E_g$ ). Also, the chemical potential of a molecule lies in the middle of  $E_g$ . Therefore, the chemical potential of a free gas of electrons is equal to its Fermi level as traditionally defined. Herein, the Fermi level of the considered systems is at the middle of  $E_g$ . All the calculations were carried out using the GAMESS suite of programs.<sup>12</sup>

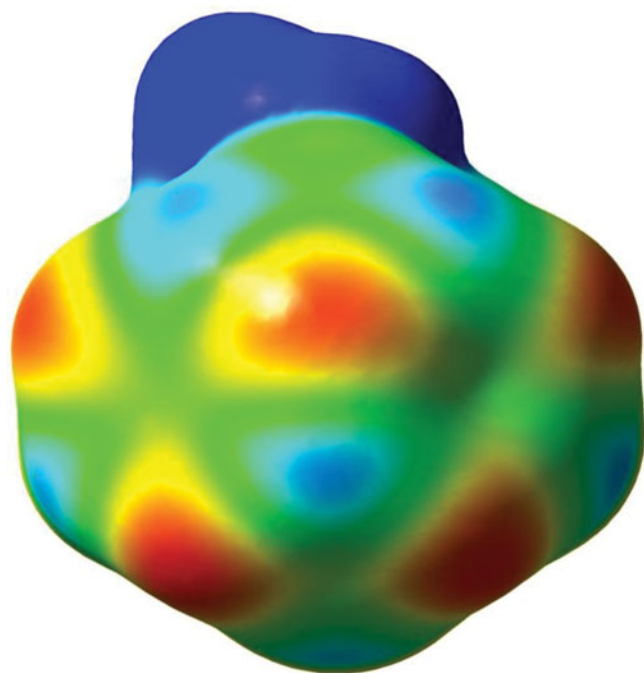
## Results and discussion

Figure 1 illustrates schematically the optimized structures, structural parameters, and calculated DOS values for pristine and Si-doped  $Al_{12}N_{12}$  nano-cages. The Al-N length for pure  $Al_{12}N_{12}$  nano-cage with  $T_h$  symmetry is about 1.858 Å in the isolated four-membered ring and 1.795 Å for square and hexagonal rings, which are in good accordance with previous

theoretical reports.<sup>13</sup>  $E_g$  and  $E_{FL}$  of an  $Al_{12}N_{12}$  nano-cage is computed to be about 3.93 eV and -4.50 eV, respectively (see Table 1).

The Mulliken population analysis reveals that about 0.746 electron charges are transferred from Al atom (with a positive charge) to its adjacent N atom within the nano-cage, suggesting an ionic character of Al-N bonds owing to a large difference in electronegativity between Al and N atoms of  $Al_{12}N_{12}$  nano-cage.<sup>9,13</sup>

Figure 2 shows various sites of a  $N_2H_4$  molecule interacting with the outer surface of  $Al_{12}N_{12}$  nano-cage at the B3LYP level of theory using 6-31G\* basis set. According to our results, binding energies ( $E_{ad}$ ) of  $N_2H_4$  molecule by the amine group to aluminum of  $Al_{12}N_{12}$  nano-cage in configurations A and B are about -1.67 eV and -1.64 eV with bond distances of 2.038 Å and 2.040 Å, respectively, which indicate mainly covalent bond character. Moreover, bonding between the  $N_2H_4$  molecule and  $Al_{12}N_{12}$  nano-cage leads to



**Figure 4.** Computed electrostatic potential surfaces of hydrazine attached to  $\text{Si}_{\text{Al}}$  model. The surfaces are defined by 0.0004 electrons/b3 contour of electronic density. Color ranges (in a.u.): blue, more positive than 0.010; green, between 0.010 and 0; yellow, between 0 and  $-0.010$ ; red, more negative than  $-0.010$ .

a charge transfer of 0.255  $|e|$  in configuration **A** and 0.244  $|e|$  in configuration **B** from the molecule to the nano-cage. These results show a significant change of local geometry for the Al-N bonds of adsorbent. The formed Al-N bonds in configurations **A** and **B** are tilted upon the outer surface of  $\text{Al}_{12}\text{N}_{12}$  nano-cage. Upon adsorption of hydrazine the Al-N bond lengths in  $\text{Al}_{12}\text{N}_{12}$  in configurations **A** and **B** increase from 1.795 Å and 1.858 Å in the pristine form (see Figure 1a) to 1.834 Å and 1.861 Å in configuration **A** and to 1.824 Å and 1.860 Å in configuration **B** (see Figure 2). For the  $\text{N}_2\text{H}_4$  molecule interacting with  $\text{Al}_{12}\text{N}_{12}$  nano-cage, the lengths of the N-N and N-H bonds are 1.449 Å and 1.024 Å in configuration **A** and 1.451 Å and 1.021 Å in configuration **B**, respectively, while the lengths of N-N and N-H bonds for an uncoordinated  $\text{N}_2\text{H}_4$  molecule are 1.487 Å and 1.023 Å, respectively.

The bond energy of hydrazine adsorbed upon the surface of g-BN sheet in water is about  $-19.7$  kcal/mol, while the bond energy of hydrazine with g-BN sheet in the most stable states in the gas phase is calculated by Beheshtian et al.<sup>9</sup> at TPSSH/6-31G\* level of theory to be  $-9.1$  kcal/mol. Our results show that adsorption of hydrazine on the  $\text{Al}_{12}\text{N}_{12}$  nano-cage is stronger than adsorption on g-BN sheet in gas phase and water. Thus, our results indicate that the pristine nano-cage can be used as a chemical adsorbent for this molecule.

As reported in literature, metal doping can improve the sensitivity of  $\text{Al}_{12}\text{N}_{12}$  nano-cage to gas molecules.<sup>8</sup> Moreover, one aluminum atom and alternatively one nitrogen atom in the six-membered ring of  $\text{Al}_{12}\text{N}_{12}$  nano-cage were replaced with one Si atom. The relaxed structural parameters of Si-doped  $\text{Al}_{12}\text{N}_{12}$  nano-cage are shown in Figure 1. The average Si-N and Si-Al bond lengths for  $\text{Si}_{\text{Al}}$  ( $\text{SiAl}_{11}\text{N}_{12}$ ) and  $\text{Si}_{\text{N}}$  ( $\text{SiAl}_{12}\text{N}_{11}$ ) models are 1.741 Å and 2.452 Å, respectively, which

is in accord with the values contained in previous reports.<sup>14,15</sup>

It can be seen that in the  $\text{Si}_{\text{N}}\text{Al}_{12}\text{N}_{11}$  nano-cage, the Si, Al, and N atoms have average Mulliken population analysis charges of  $-0.250$ ,  $0.569$ , and  $-0.761 |e|$ , respectively, while for the  $\text{Si}_{\text{Al}}\text{Al}_{11}\text{N}_{12}$  nano-cage the corresponding charges are  $0.895$ ,  $0.608$ , and  $-0.761 |e|$ , respectively. Upon adsorption the average MPA charges for Si, Al, and N atoms of  $\text{Si}_{\text{N}}\text{Al}_{12}\text{N}_{11}$  nano-cage change to  $-0.249$ ,  $0.490$ , and  $-0.758 |e|$ , respectively, while for  $\text{Si}_{\text{Al}}\text{Al}_{11}\text{N}_{12}$  nano-cage the corresponding charges are  $-0.250$ ,  $0.569$ , and  $-0.761 |e|$ , respectively. The charge of Si atom is negative in  $\text{Si}_{\text{N}}$  and  $\text{Si}_{\text{Al}}$  models. The computed bond energies ( $E_{\text{ad}}$ ) of all possible initial models are shown in Table 1.

As shown in Figure 3, the high exothermic bond energies for configurations **A** and **B** in the  $\text{Si}_{\text{Al}}$  model are calculated to  $-1.18$  eV and  $-1.23$  eV with the bond lengths of 1.972 Å and 1.973 Å, respectively. For configuration **A**, the lengths of N-N and N-H bonds of the  $\text{N}_2\text{H}_4$  molecule are 1.449 Å and 1.026 Å and for configuration **B**, the bond lengths are 1.446 Å and 1.024 Å respectively.

For configurations **A** and **B** the charges transferred from an  $\text{N}_2\text{H}_4$  molecule to adsorbent are 0.221  $|e|$  and 0.272  $|e|$ , respectively. In the  $\text{Si}_{\text{N}}$  model, as shown in Figure 3, the low exothermic bond energy and the bond length in configuration **C** are  $-0.30$  eV and 2.431 Å, respectively, which are much smaller than in the  $\text{Si}_{\text{Al}}$  model. This demonstrates that the bond energy values for the  $\text{Si}_{\text{Al}}$  model are energetically remarkable for the adsorption of  $\text{N}_2\text{H}_4$  molecule. The charge transfer from an  $\text{N}_2\text{H}_4$  molecule to adsorbent is 0.207  $|e|$ .

As shown in Figure 4, the MEP map for  $\text{N}_2\text{H}_4$  molecule attached to the  $\text{Si}_{\text{Al}}$  model in  $\text{SiAl}_{11}\text{N}_{12}$  nano-cage was studied. The calculated MEP map for this system indicates that the  $\text{N}_2\text{H}_4$  molecule acts as an electron donor (positively charged, blue color) and the Si-doped  $\text{Al}_{12}\text{N}_{12}$  nano-cage acts as an electron acceptor (negatively charged, red color).

The energy of the highest occupied molecular orbital (HOMO) and that of the lowest unoccupied molecular orbital (LUMO) as well as the energy gap between them are computed at the B3LYP/6-31G\* level of theory to evaluate the energetic behavior of the studied systems. The energies and the representation of the HOMO and LUMO orbitals are shown in Table 1 and Figure 5, respectively. The positive and negative phases are represented in red and green colors, respectively. Figure 5 explains the fact that charge transfer interaction is taking place between the nano-cages and the  $\text{N}_2\text{H}_4$  molecule. Generally, the HOMO and LUMO molecular orbitals play an important role in the chemical activity of molecules. We calculated the energies of HOMO and LUMO in the most stable configurations for the  $\text{N}_2\text{H}_4$  molecule interacting with  $\text{Si}_{\text{Al}}$  and  $\text{Si}_{\text{N}}$  sites in nano-cages. The energies of HOMO and LUMO are  $-3.11$  eV and  $-1.57$  eV in configuration **A** and  $-3.45$  eV and  $-2.04$  eV in configuration **B** for  $\text{Si}_{\text{Al}}$  model, and  $-4.64$  eV and  $-2.12$  eV for  $\text{Si}_{\text{N}}$  model (see Table 1), while the energies of HOMO and LUMO are  $-4.68$  eV and  $-2.42$  eV for  $\text{Si}_{\text{Al}}\text{Al}_{11}\text{N}_{12}$  nano-cage and  $-5.88$  eV and  $-2.47$  eV for  $\text{Si}_{\text{N}}\text{Al}_{12}\text{N}_{11}$  nano-cage. Therefore, the adsorption of  $\text{N}_2\text{H}_4$  molecule leads to a significant change in the HOMO energy in comparison with the LUMO energy.

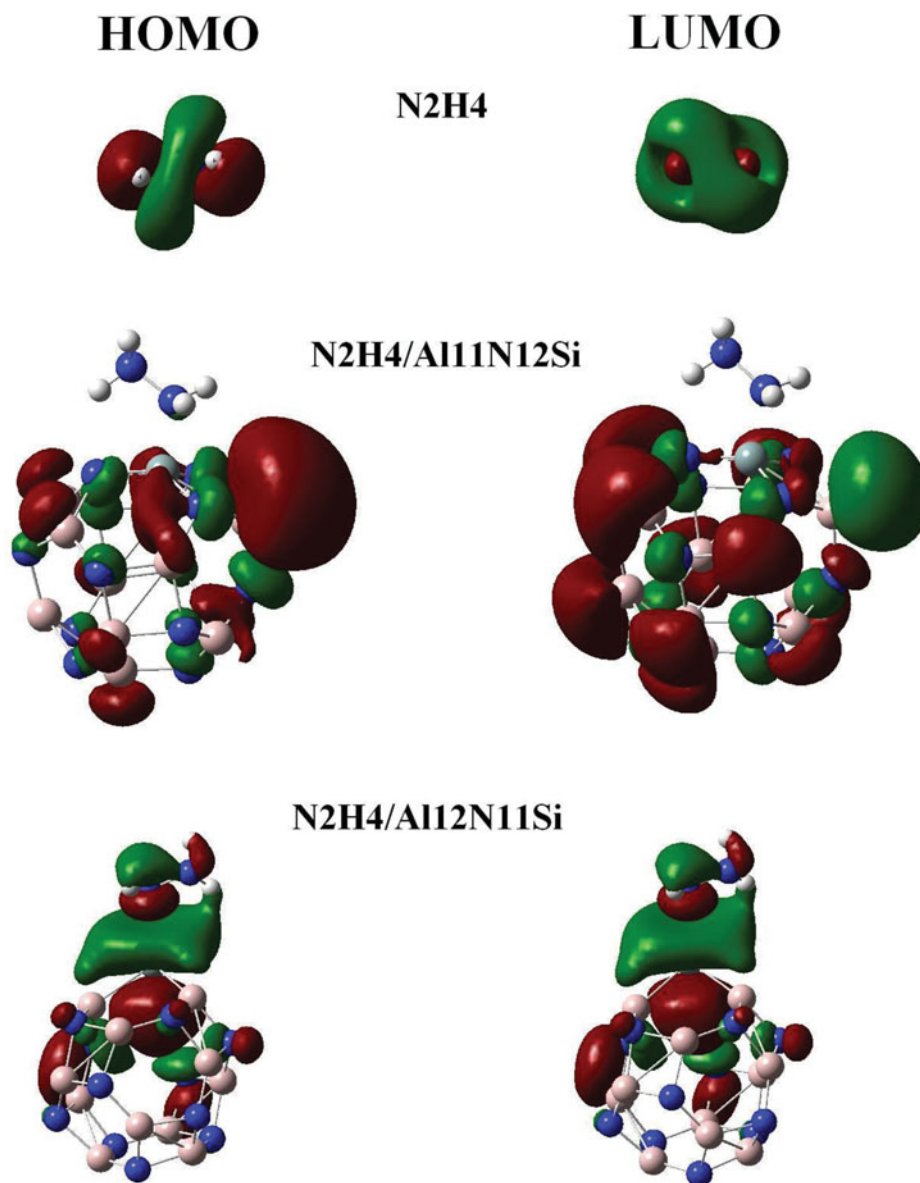


Figure 5. HOMO and LUMO orbitals for different systems.

Table 2. Calculated thermodynamic properties [ $\Delta H$ ,  $\Delta G$  (kJ/mol) and  $\Delta S$  (J/mol K)] as well as minimum and maximum vibrational frequencies ( $\text{cm}^{-1}$ ) for the considered systems.

Structure	$\Delta H_{\text{ad}}$	$\Delta G_{\text{ad}}$	$\Delta S_{\text{ad}}$	$\nu_{\text{min}}$	$\nu_{\text{max}}$
$\text{Al}_{12}\text{N}_{12}$	–	–	–	155.84	938.94
$\text{SiAl}_{11}\text{N}_{12}$	–	–	–	154.49	955.93
$\text{SiAl}_{12}\text{N}_{11}$	–	–	–	119.57	947.83
$\text{N}_2\text{H}_4/\text{Al}_{12}\text{N}_{12}$ (Figure 2a)	–36.71	–26.49	–34.28	43.48	3533.59
$\text{N}_2\text{H}_4/\text{Al}_{12}\text{N}_{12}$ (Figure 2b)	–36.26	–25.86	–34.90	58.69	3510.95
$\text{N}_2\text{H}_4/\text{SiAl}_{11}\text{N}_{12}$ (Figure 3a)	–25.67	–15.04	–35.64	62.93	3539.22
$\text{N}_2\text{H}_4/\text{SiAl}_{11}\text{N}_{12}$ (Figure 3b)	–26.18	–14.64	–38.70	56.52	3542.68
$\text{N}_2\text{H}_4/\text{SiAl}_{12}\text{N}_{11}$ (Figure 3c)	–5.45	3.68	–30.63	22.98	3553.04

For better understanding of electronic properties, DOS plots for the interaction of  $N_2H_4$  with pristine and Si-doped  $Al_{12}N_{12}$  nano-cages were calculated. For  $N_2H_4$  adsorption on  $Si_{Al}Al_{11}N_{12}$  nano-cage, the DOS plot reveals that the energy gap is reduced from 2.26 eV in pristine  $Si_{Al}Al_{11}N_{12}$  to 1.54 eV in configuration **A** and 1.41 eV in configuration **B** in  $N_2H_4/Si_{Al}Al_{11}N_{12}$  model (see Table 1). The essential sensing mechanisms in nano-structure devices are a change in  $E_g$  of nano-structure and subsequently a change in its conductivity upon the adsorption process.<sup>16</sup> As shown in Table 1, the energy gap of  $Si_{Al}Al_{11}N_{12}$  nano-cage is significantly changed on the adsorption of  $N_2H_4$  molecule ( $\Delta E_g = -31.86\%$  and  $-37.61\%$  for configurations **A** and **B** in  $Si_{Al}$  model, respectively). The changes lead to a considerable increase in the electrical conductivity of nano-cage. The behavior can be explained according to the following equation<sup>17</sup>:

$$\sigma \propto \exp\left(\frac{-E_g}{2kT}\right). \quad \text{Eq. (4)}$$

In this equation,  $\sigma$  is the electric conductivity of the structure and  $k$  is the Boltzmann's constant. According to the above-mentioned equation, smaller  $E_g$  at a specific temperature leads to a larger electric conductivity. Therefore, considerable change in  $E_g$  of nano-cage shows that  $Si_{Al}Al_{11}N_{12}$  may be a very good  $N_2H_4$  sensor. On the other hand, it is well known that one of the most important factors in sensor devices is their recovery time ( $\tau$ ), which can be described as follows:

$$\tau = \nu_0^{-1} \exp(-E_{ad}/k_B T). \quad (5)$$

Here  $k_B$  is the Boltzmann's constant,  $T$  is the temperature, and  $\nu_0$  is the frequency used. According to the above-mentioned equation, more negative  $E_{ad}$  will prevent the recovery of device. In other words, very strong interactions are not favorable in gas sensor devices due to long recovery periods ( $\tau$ ). As shown in Table 1, the  $E_{ad}$  value in configurations **A** and **B** are  $-1.18$  eV and  $-1.23$  eV, indicating that the  $Si_{Al}Al_{11}N_{12}$  nano-cage has a strong interaction with the  $N_2H_4$  molecule and will prevent the recovery of device. But in the  $Si_N$  or  $N_2H_4/Si_{Al}Al_{12}N_{11}$  model,  $E_g$  of the nano-cage is reduced from 3.41 eV in pristine  $Si_NAl_{12}N_{11}$  nano-cage to 2.52 eV in configuration **C** of  $N_2H_4/Si_{Al}Al_{12}N_{11}$  model ( $\Delta E_g = -26.10\%$ ). The considerable change in  $E_g$  of nano-cage shows that  $Si_NAl_{12}N_{11}$  is very sensitive toward  $N_2H_4$  molecules. On the other hand, the  $E_{ad}$  value of configuration **C** is about  $-0.30$  eV (see Table 1), which is not too large to hinder the recovery of nano-cage. Also, for the configurations it can be found that DOS near the Fermi level are affected by the adsorption of  $N_2H_4$  molecule. Therefore,  $Si_NAl_{12}N_{11}$  can be a useful sensor for detection of hydrazine.

In order to investigate the thermodynamic feasibility of  $N_2H_4$  adsorption on pristine and Si-doped  $Al_{12}N_{12}$  nano-cages, changes in enthalpies ( $\Delta H_{ad}$ ), free energies ( $\Delta G_{ad}$ ), and entropies ( $\Delta S$ ) of configurations at 298.14 K and 1 atmosphere are calculated from the frequency calculations according to Equations (6)–(8), and are summarized in Table 2.

$$\Delta H_{ad} = H_{N_2H_4/Al_{12}N_{12}} - H_{N_2H_4} - H_{Al_{12}N_{12}} \quad (6)$$

$$\Delta S_{ad} = S_{N_2H_4/Al_{12}N_{12}} - S_{N_2H_4} - S_{Al_{12}N_{12}} \quad (7)$$

$$\Delta G_{ad} = G_{N_2H_4/Al_{12}N_{12}} - G_{N_2H_4} - G_{Al_{12}N_{12}} \quad (8)$$

Calculated frequencies are positive, showing that the structures are stable. Calculated values of  $\Delta H_{ad}$  and  $\Delta G_{ad}$  for configurations **A** and **B** in Figures 2 and 3 show a strong interaction between  $N_2H_4$  molecule and pristine as well as Si-doped  $Al_{12}N_{12}$  nano-cages (see Table 2). The results again show that  $Al_{12}N_{12}$  nano-cage can be a promising candidate for adsorption of hydrazine from environmental systems, whereas  $\Delta H_{ad}$  and  $\Delta G_{ad}$  for configuration **C** in Figure 3 show a weak interaction between  $N_2H_4$  molecule and  $Si_{Al}Al_{12}N_{11}$  nano-cage. Therefore, the structure shows no strong interaction with  $N_2H_4$  molecule that prevents the recovery of device.

## Conclusions

The results obtained in the present study indicate that the adsorption of hydrazine on the surface of  $Al_{12}N_{12}$  nano-cage is energetically notable and its electronic structure changes slightly on adsorption. Our results show that  $Al_{12}N_{12}$  nano-cage can be introduced as a chemical adsorbent for toxic hydrazine in nature. From the computed results for hydrazine interacting with Si-doped  $Al_{12}N_{12}$  nano-cage, the adsorption of hydrazine at  $Si_{Al}$  and  $Si_N$  sites of the nano-cage can significantly improve the sensitivity of the nano-cage to hydrazine. On the other hand, the  $E_{ad}$  value of  $Si_N$  is about  $-0.30$  eV, which is not too large to hinder the recovery of the nano-cage. Therefore, the calculations show that  $Si_NAl_{12}N_{11}$  can be a useful sensor for detection of hydrazine.

## References

1. Ensafi, A. A.; Mirmomtaz, E. *J. Electroanal. Chem.* **2005**, 583, 176–183.
2. Augusta, M. K.; Diño, W. A.; David, M.; Nakanishi, H.; Kasai, H. *Surf. Sci.* **2010**, 604, 245–251.
3. Augusta, M. K.; Kasai, H. *Surf. Sci.* **2012**, 606, 766–771.
4. Zhang, P.-X.; Wang, Y.-G.; Huang, Y.-Q.; Zhang, T.; Wu, G.-S.; Li, J. *Catalysis Today* **2011**, 165, 80–88.
5. Alberas, D. J.; Kiss, J.; Liu, Z.-M.; White, J. M. *Surf. Sci.* **1992**, 278, 51–61.
6. Yu, M.; Tian, W. Q.; Jayanthi, C. S.; Wu, S. Y. *Chem. Phys. Lett.* **2011**, 518, 93–98.
7. Beheshtian, J.; Ahmadi Peyghan, A.; Bagheri, Z. *Struct. Chem.* **2013**, 24, 1565–1570.
8. Soltani, A.; Ghafouri Raz, S.; Ramezani Taghartapeh, M.; Varasteh Moradi, A.; Zafar Mehrabian, R. *Comput. Mater. Sci.* **2013**, 79, 795–803.
9. Beheshtian, J.; Peyghan, A. A.; Bagheri, Z. *Comp. Mater. Sci.* **2012**, 62, 71–74.
10. Baei, M. T.; Moradi, A. V.; Moghimi, M.; Torabi, P. *Comp. Theor. Chem.* **2011**, 967, 179–184.
11. Beheshtian, J.; Baei, M. T.; Peyghan, A. A. *Surf. Sci.* **2012**, 606, 981–985.
12. Schmidt, M. W.; Baldrige, K. K.; Boatz, J. A.; Elbert, S. T.; Gordon, M. S.; Jensen, J. H.; Koseki, Sh.; Matsunaga, N.; Ngyen, K. A.; Su, Sh.; Windus, Th. L.; Dupuis, M.; Montgomery Jr., J. A. *J. Comput. Chem.* **1993**, 14, 1347–1363.
13. Wang, Q.; Sun, Q.; Jena, P.; Kawazoe, Y. *ACS NANO* **2009**, 3, 621–626.
14. Baei, M. T.; Hashemian, S.; Yourdkhani, S. *Superlattices Microstruct.* **2013**, 60, 437–442.
15. Wang, R.; Zhu, R.; Zhang, D. *Chem. Phys. Lett.* **2008**, 467, 131–135.
16. Zhou, X.; Tian, W. Q.; Wang, X.-L. *Sens. Actuators B* **2010**, 151, 56–64.
17. Li, S. *Semiconductor Physical Electronics*, 2nd ed.; Springer: New York, NY, **2006**.